Double-resonance frequency shift in a hydrogen maser

M. A. Humphrey, D. F. Phillips, and R. L. Walsworth

Harvard-Smithsonian Center for Astrophysics, Cambridge, Massachusetts 02138
(Received 16 July 2000; published 14 November 2000)

We use the dressed-atom formalism to calculate the frequency shift in a hydrogen maser induced by applied radiation near the Zeeman frequency, and find excellent agreement with a previous calculation made in the bare-atom basis. The maser oscillates on the $\Delta F = 1$, $\Delta m_F = 0$ hyperfine transition, while the applied field is swept through the $F = 1$, $\Delta m_F = \pm 1$ Zeeman resonance. We determine the effect of the applied field on the Zeeman levels using the dressed-atom picture, and then calculate the maser frequency shift by coupling the dressed states to the microwave cavity. Qualitatively, the dressed-atom analysis gives a simpler physical interpretation of this double-resonance process, which has applications in precision hydrogen Zeeman spectroscopy, e.g., in fundamental symmetry tests.

PACS number(s): 32.60.+i, 32.80.Wr

I. INTRODUCTION

Since its development nearly 40 years ago, the hydrogen maser has served as a robust tool capable of making high-precision measurements by utilizing its excellent frequency stability [1–3]. Hydrogen masers are currently the most stable active oscillators over intervals of seconds to days, with applications including very long baseline interferometry, deep-space tracking and navigation, and metrology. In addition, hydrogen masers have been used to make precision atomic physics measurements [4–8] and for sensitive tests of general relativity [9] and quantum mechanics [10,11].

A hydrogen maser operates on the first-order magnetic field-independent $\Delta F = 1$, $\Delta m_F = 0$ hyperfine transition, between states $|2\rangle$ and $|4\rangle$ of the electronic ground state (see Fig. 1). As shown in Fig. 2, atoms in states $|1\rangle$ and $|2\rangle$ are injected into a storage bulb residing in a microwave cavity tuned near the hyperfine frequency, creating the population inversion necessary for active maser oscillation. The microwave field stimulates a small, coherent magnetization in the atomic ensemble, and this magnetization acts as a source to increase the microwave field. With sufficiently high atomic flux and low cavity losses, this feedback induces active maser oscillation. The maser frequency is very stable; a well engineered hydrogen maser can have fractional frequency stability on the order of 1×10^{-15} over intervals of a few hours.

Hydrogen masers can also be used as sensitive probes of the $F = 1$, $\Delta m_F = \pm 1$ Zeeman resonances through a double-resonance technique [12], in which an oscillating magnetic field tuned near the atomic Zeeman resonance shifts the $\Delta F = 1$, $\Delta m_F = 0$ maser frequency. At low static magnetic fields, this maser frequency shift is an antisymmetric function of the detuning of the applied oscillating field from the Zeeman resonance. Thus, by observing the antisymmetric pulling of the otherwise stable maser frequency, the hydrogen Zeeman frequency can be determined with high precision.

An early investigation of atomic double resonance was made by Ramsey [13], who calculated the frequency shift between two levels coupled by radiation to other levels. This calculation treated the problem perturbatively to first order in

the coupling field strength, and it neglected damping. Later, Andresen [12,14] calculated the frequency shift in a hydrogen maser due to an applied field oscillating near the $F = 1$ Zeeman frequency (see Sec. II), and then measured this double-resonance effect using a hydrogen maser, finding reasonable agreement with the calculation. Andresen's calculation employed a bare-atom basis, treating the problem to second order in the applied field strength, and including phenomenological damping terms, but used an oversimplified description of spin-exchange relaxation. Savard *et al.* [15] revisited the problem with a more realistic spin-exchange relaxation description [16], and found a small correction to the earlier work.

Although the work of Andresen and Savard *et al.* provides a complete description of the double-resonance maser frequency shift, intuitive understanding is obscured by the length of the calculations and the use of the bare-atom basis. In particular, these works demonstrated that the amplitude of the antisymmetric maser frequency shift is directly proportional to the electronic polarization of the masing atomic ensemble. The maser frequency shift vanishes as this polar-
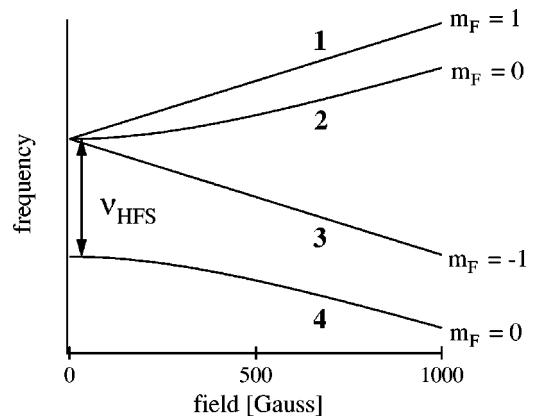

FIG. 1. Hydrogen hyperfine structure. A hydrogen maser oscillates on the first-order magnetic field-independent $|2\rangle \leftrightarrow |4\rangle$ hyperfine transition near 1420 MHz. The maser typically operates with a static field less than 1 mG. For these low-field strengths, the two $F = 1$, $\Delta m_F = 1$ Zeeman frequencies are nearly degenerate, and $\nu_{12} \approx \nu_{23} \approx 1$ kHz.
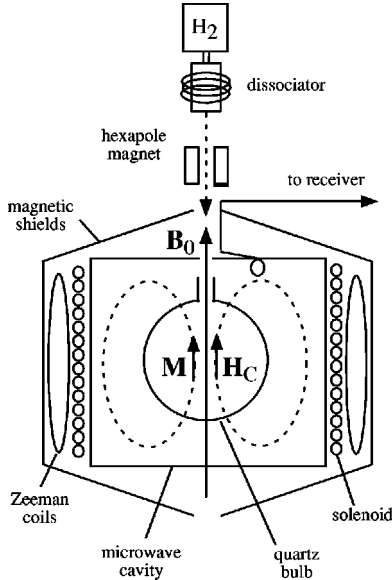
FIG. 2. Hydrogen maser schematic. The solenoid generates a weak static magnetic field $\mathbf{B}_0$ which defines a quantization axis inside the maser bulb. The microwave cavity field $\mathbf{H}_C$ (dashed field lines) and the coherent magnetization $\mathbf{M}$ of the atomic ensemble form the coupled actively oscillating system.

ization goes to zero. The previous bare-atom analyses provide no physical interpretation of this effect.

Since the dressed-atom formalism [17] often adds physical insight to the understanding of the interaction of matter and radiation, here we apply it to the double-resonance frequency shift in a hydrogen maser. In a two-step process, we first use the dressed-atom picture to determine the effect of the applied Zeeman radiation on the atomic states. Then we analyze the effect of the microwave cavity field on the dressed states, and determine the maser frequency shift. We find excellent quantitative agreement between the dressed-atom calculation and the previous bare-atom result. We exploit the dressed-atom calculation to offer a simple physical interpretation of the double-resonance hydrogen maser frequency shift, including a straightforward explanation of the polarization dependence. We conclude by noting the experimental application of the double-resonance effect to perform improved, high precision hydrogen Zeeman spectroscopy.

II. MASER OSCILLATION FREQUENCY

In a hydrogen maser (Fig. 2), molecular hydrogen is dissociated in a rf discharge, and a thermal beam of hydrogen atoms is formed. A hexapole state selecting magnet focuses the higher-energy, low-field-seeking hyperfine states ($|1\rangle$ and $|2\rangle$) into a quartz maser bulb at about 10^{12} atoms/sec. Inside the bulb (volume $\approx 10^3$ cm^3), the atoms travel ballistically for about 1 sec before escaping, making $\approx 10^4$ collisions with the bulb wall. A Teflon coating reduces the atom-wall interaction, and thus inhibits decoherence of the masing atomic ensemble by wall collisions. The maser bulb is centered inside a cylindrical TE$_{011}$ microwave cavity resonant with the 1420-MHz hyperfine transition. As described above, the microwave field and atomic ensemble form a

coupled system with positive feedback that will actively oscillate near the $\Delta F = 1$, $\Delta m_F = 0$ hyperfine frequency if there is a sufficiently high atomic flux into the maser bulb. Since the atoms are confined to a region of uniform microwave field phase, their velocity is effectively averaged to zero over the interaction time with the microwave field, and first-order Doppler effects are eliminated. The maser signal is inductively coupled out of the microwave cavity, and amplified with an external receiver. Surrounding the cavity, a solenoid produces a weak static magnetic field to maintain the quantization axis inside the maser bulb, and a pair of Helmholtz coils produces the oscillating transverse magnetic field that drives the $F = 1$ Zeeman transitions. The cavity, solenoid, and Zeeman drive coils are all enclosed within several layers of magnetic shielding.

To calculate the maser oscillation frequency, we first determine the relationship between the microwave field and a source magnetization. If we assume that a single-cavity mode is dominant within the microwave cavity, we may write the microwave magnetic field oscillating at frequency ω as $\mathbf{H}(\mathbf{r},\omega) = \sqrt{4\pi} p_C(\omega) \mathbf{H}_C(\mathbf{r})$, where p_C characterizes the frequency- (i.e. time-) dependent amplitude and $\mathbf{H}_C$ represents the time-independent spatial variation of the mode. A straightforward application of Maxwell's equations relates $p_C(\omega)$ to a source magnetization $M(\omega)$,

$$\left(\omega_C^2 + \frac{i\omega_C\omega}{Q_C} - \omega^2 \right) p_C(\omega) = \sqrt{4\pi} \omega^2 \langle H_C^{(z)} \rangle_b V_b M(\omega),$$
(1)

where ω is the maser frequency, ω_C is the cavity frequency, $\langle H_C^{(z)} \rangle_b$ is the average of the microwave field's z component over the bulb, and V_b is the volume of the maser bulb. The second term on the left has been introduced phenomenologically to account for cavity losses characterized by Q_C, the cavity quality factor. The source magnetization is produced by the atomic ensemble, and is given by the expectation value of the magnetic dipole operator (neglecting the term precessing at $-\omega$),

$$M(\omega) = N\langle \hat{\mu} \rangle = N\,\mathrm{Tr}(\hat{\rho}\hat{\mu}) = N\mu_{24}\rho_{42}(\omega),$$
(2)

where N is the atomic density and μ_{24} is the hyperfine transition dipole matrix element, and $\mu_{24} \approx -\mu_B$ (where μ_B is the Bohr magneton). The atomic coherence $\rho_{42}(\omega)$ is found by solving the Bloch equations

$$\dot{\rho} = \frac{i}{\hbar}[\rho, H_0] + \frac{i}{\hbar}[\rho, H_{int}] + \dot{\rho}_{flux} + \dot{\rho}_{relax}$$
(3)

in the steady state. The unperturbed Hamiltonian H_0 includes only the atomic state energies (given by the hyperfine and Zeeman interactions), and the interaction Hamiltonian H_{int} describes the effect of the microwave cavity field, which couples states $|2\rangle$ and $|4\rangle$. For perfect hexapole state selection, the flux term is written

$$\dot{\rho}_{flux} = \frac{r}{2}(|1\rangle\langle 1| + |2\rangle\langle 2|) - r\rho,$$
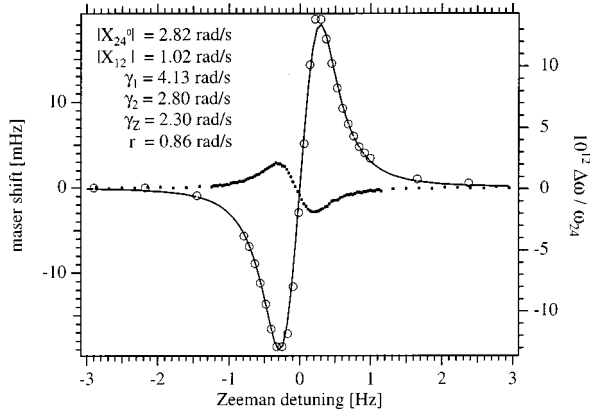(4)

FIG. 3. Double-resonance maser frequency shifts. The large open circles are data taken with an input beam of $|2\rangle$ and $|3\rangle$ hydrogen atoms. These are compared with Eq. (6) (full curve) using the parameter values shown. The values of $|X_{12}|$ and γ_Z were chosen to fit the data, while the remaining parameters were independently measured. The experimental error of each measurement is smaller than the circle marking it. The electronic polarization dependence of the double-resonance effect is illustrated with the dotted data points: with an input beam of $|1\rangle$ and $|2\rangle$ atoms, the shift is inverted. (The dotted points were acquired with a weaker applied Zeeman field, resulting in smaller maser frequency shifts.) The large variation of the maser frequency shift with Zeeman detuning near resonance, along with the excellent maser frequency stability, allows the Zeeman frequency (≈ 800 Hz) to be determined to about 3 mHz in a single scan of the double resonance (requiring ≈ 20 min of data acquisition).

where the positive terms account for the injection of atoms in states $|1\rangle$ and $|2\rangle$ at rate r, and the last term accounts for bulb escape. The relaxation term $\dot{\rho}_{relax}$ phenomenologically describes population and coherence relaxation due to wall collisions, magnetic-field inhomogeneities, and spin-exchange collisions.

In the absence of Zeeman radiation and for small detuning of the cavity from the $|2\rangle \leftrightarrow |4\rangle$ hyperfine transition frequency, ω_{24}, the maser frequency is found using Eqs. (1)–(3), to be

$$\omega = \omega_{24} + \frac{Q_C}{Q_l}(\omega_C - \omega_{24}), \qquad (5)$$

where $Q_l = \omega_{24}/\Delta\omega$, the atomic line-Q, is on the order of 10^9 [1]. Since the cavity-Q is on the order of 10^4, the cavity pulling is highly suppressed, and the maser oscillates near the atomic hyperfine frequency, ω_{24}.

In the presence of Zeeman radiation, the maser frequency is shifted, as first shown by Andresen [12] and measured anew here (see Fig. 3). Andresen's calculation of the double-resonance shift included the applied Zeeman field in the interaction Hamiltonian, but otherwise left unchanged the above analysis for the maser frequency. To second order in the Rabi frequency of the applied Zeeman field, $|X_{12}|$, and in terms of the unperturbed maser Rabi frequency $|X_{24}^0|$, atom flow rate r, population decay rate γ_1, hyperfine decoherence rate γ_2, and Zeeman decoherence rate γ_Z, the small static field limit of the maser shift is given by [18]

$$\Delta\omega = -|X_{12}|^2 \frac{\gamma_Z}{r}(\gamma_1\gamma_2 + |X_{24}^0|^2)$$

$$\times \frac{\delta(\rho_{11}^0 - \rho_{33}^0)}{(\gamma_Z^2 - \delta^2 + \frac{1}{4}|X_{24}^0|^2)^2 + (2\delta\gamma_Z)^2}, \qquad (6)$$

where δ is the detuning of the applied field from the atomic Zeeman frequency, and $\rho_{11}^0 - \rho_{33}^0 = r/(2\gamma_1)$ is the steady-state population difference between states $|1\rangle$ and $|3\rangle$ in the absence of an applied Zeeman field (following Eq. (8) of Ref. [12]). Physically, the population difference between states $|1\rangle$ and $|3\rangle$ represents the electronic polarization of the hydrogen ensemble [14]:

$$P = \frac{\langle S_Z\rangle}{S} = 2\,\mathrm{Tr}(\hat{\rho}\hat{S}_Z) = \rho_{11} - \rho_{33}. \qquad (7)$$

Equation (6) implies that a steady-state electronic polarization, and hence a population difference between states $|1\rangle$ and $|3\rangle$ injected into the maser bulb, is a necessary condition for the maser to exhibit a double-resonance frequency shift. Walsworth *et al.* demonstrated this polarization dependence experimentally by operating a hydrogen maser in three configurations: (i) with the usual input flux of atoms in states $|1\rangle$ and $|2\rangle$; (ii) with a pure input flux of atoms in state $|2\rangle$, where the maser frequency shift vanishes; and (iii) with an input beam of atoms in states $|2\rangle$ and $|3\rangle$, where the maser shift is inverted [7].

For typical applied Zeeman field strengths, the 1420-MHz maser frequency is shifted tens of mHz (see Fig. 3), a fractional shift of $\approx 10^{-11}$. However, the shift is easily resolved because of the excellent fractional maser frequency stability (parts in 10^{15}).

III. DRESSED-ATOM CALCULATION

We now consider an alternative approach to calculating the double-resonance maser frequency shift using the dressed-atom picture. We retain the Maxwell-Bloch formalism of Eqs. (1)–(3); however, we determine the steady-state coherence $\rho_{42}(\omega)$ in a dressed-atom basis, including the atomic state energies, the applied Zeeman field, and the atom-Zeeman field interaction. For simplicity, we assume the static magnetic field is sufficiently low that the two $F=1$, $\Delta m_F = \pm 1$ Zeeman frequencies are nearly degenerate, $\omega_{12} - \omega_{23} \ll \gamma_Z$, as is the case for typical hydrogen maser operation. We use the simplified spin-exchange relaxation model [12], and neglect the small spin-exchange correction to the double-resonance maser frequency shift [15].

A. Dressed-atom basis

By incorporating the applied Zeeman field into the unperturbed Hamiltonian, it takes the form $H_0 = H_a + H_f + V_{af}$. The atomic states (defining state $|2\rangle$ as energy zero) are described by $H_a = \hbar\omega_{12}|1\rangle\langle 1| - \hbar\omega_{23}|3\rangle\langle 3| - \hbar\omega_{24}|4\rangle\langle 4|$; the

applied Zeeman field (at frequency ω_Z) is described by $H_f = \hbar \omega_Z a^\dagger a$; and the interaction between them is given by

$$V_{af} = \hbar g (a + a^\dagger)[|1\rangle\langle2| + |2\rangle\langle3| + \text{H.c.}]. \qquad (8)$$

Here the Zeeman field creation and annihilation operators are $a^\dagger$ and a, H.c. denotes the Hermitian conjugate, and g is the single-photon Rabi frequency for the Zeeman transitions. We will use eigenkets with two indices to account for the atomic state and the number of photons in the Zeeman field, denoted by n. We select four of these as our bare atom-Zeeman field basis, $\{|1,n-1\rangle, |2,n\rangle, |3,n+1\rangle, |4,n\rangle\}$, where the first entry indicates the atomic state and the second entry indicates the Zeeman photon number. We note that for a resonant field, $\omega_Z = \omega_{12}$, the first three basis states are degenerate. Also, $n \gg 1$ in practice for there to be any measurable double-resonance maser frequency shift.

In this bare-atom–Zeeman field basis, the unperturbed Hamiltonian operator takes the matrix form

$$H_0 = \hbar \begin{pmatrix} -\delta & \frac{1}{2}X_{12} & 0 & 0 \\ \frac{1}{2}X_{12} & 0 & \frac{1}{2}X_{23} & 0 \\ 0 & \frac{1}{2}X_{23} & \delta & 0 \\ 0 & 0 & 0 & -\omega_{24} \end{pmatrix}, \qquad (9)$$

where $\delta = \omega_Z - \omega_{12}$ is the detuning of the applied Zeeman field, and

$$\frac{X_{12}}{2} = g\sqrt{n} \approx g\sqrt{n+1} = \frac{X_{23}}{2} \qquad (10)$$

define the Zeeman field Rabi frequency (the factor of 2 has been inserted to be consistent with our rotating-wave-approximation convention; see Ref. [18]). By diagonalizing H_0, we find basis states which physically represent the atomic states dressed by the applied Zeeman field. The dressed-energy levels are the eigenvalues of H_0: $E_a = \hbar\Omega$, $E_b = 0$, $E_c = -\hbar\Omega$, and $E_4 = -\hbar\omega_{24}$, where $\Omega = \sqrt{\delta^2 + \frac{1}{2}X_{12}^2}$ represents the generalized Rabi frequency. The dressed states are the eigenvectors of H_0:

$$|a\rangle = \frac{1}{2}\left(1 - \frac{\delta}{\Omega}\right)|1,n-1\rangle + \frac{X_{12}}{2\Omega}|2,n\rangle + \frac{1}{2}\left(1 + \frac{\delta}{\Omega}\right)|3,n+1\rangle,$$

$$|b\rangle = \frac{X_{12}}{2\Omega}|1,n-1\rangle + \frac{\delta}{\Omega}|2,n\rangle - \frac{X_{12}}{2\Omega}|3,n+1\rangle,$$

$$(11)$$

$$|c\rangle = \frac{1}{2}\left(1 + \frac{\delta}{\Omega}\right)|1,n-1\rangle - \frac{X_{12}}{2\Omega}|2,n\rangle + \frac{1}{2}\left(1 - \frac{\delta}{\Omega}\right)|3,n+1\rangle,$$

$$|4\rangle = |4,n\rangle.$$

Note that in the limit of large negative δ, $|a\rangle \to |1\rangle$ and $|c\rangle \to |3\rangle$, while in the limit of large positive δ, $|a\rangle \to |3\rangle$ and

$|c\rangle \to |1\rangle$. This will become important in the physical interpretation of the maser frequency shift (see Sec. IV).

An operator $\hat{O}$ transforms between bare- and dressed-atom bases as $\hat{O}^d = T^{-1}\hat{O}^b T$, where T is the unitary matrix linking the dressed- and bare-atom basis states [coefficients of Eq. (11)]. The dressed- and bare-atom energies and eigenvectors are equivalent for the $F=0$ hyperfine state $|4\rangle$ because this state is unaffected by the applied Zeeman field.

B. Dressed-basis Bloch equations

We now couple the dressed states to the microwave cavity using the Bloch equations, which remain of the form

$$\dot{\rho}^d = \frac{i}{\hbar}[\rho^d, H_0^d] + \frac{i}{\hbar}[\rho^d, H_{int}^d] + \dot{\rho}_{relax}^d + \dot{\rho}_{flux}^d. \qquad (12)$$

The unperturbed Hamiltonian H_0 now accounts for the bare-atom energies and the applied Zeeman driving field, while the microwave cavity field is included in the interaction Hamiltonian H_{int}. Since the dressed states $|a\rangle, |b\rangle$, and $|c\rangle$ all have a component of the atomic state $|2\rangle$ [see Eq. (11)], the microwave field couples state $|4\rangle$ to each:

$$H_{int}^d = \frac{X_{12}}{2\Omega}H_{24}|a\rangle\langle4| + \frac{\delta}{\Omega}H_{24}|b\rangle\langle4|$$

$$- \frac{X_{12}}{2\Omega}H_{24}|c\rangle\langle4| + \text{H.c.} \qquad (13)$$

Note that $H_{24} = \langle2|\hat{\boldsymbol{\mu}} \cdot \mathbf{H}_C|4\rangle$ is the only nonzero coupling between bare-atom states supported by the TE$_{011}$ mode microwave cavity. To transform the relaxation terms into the dressed basis, we make the approximation that all relaxation rates (population decay γ_1, hyperfine decoherence γ_2, and Zeeman decoherence γ_Z) have the same value, $\gamma + r$ (γ includes all relaxation exclusive of bulb loss). Typically, these rates are within a factor of 2 (see the values listed in Fig. 3). Then,

$$\dot{\rho}_{relax}^d = -\gamma\rho^d + \frac{\gamma}{4}\mathbb{1}. \qquad (14)$$

In the bare-atom basis, the flux term has a very simple form [Eq. (4)] with no off-diagonal input entries since the injected beam has no coherence between the bare atomic states. In the dressed basis, however, there is an injected Zeeman coherence, so the flux term takes a considerably more complicated form,

$$\dot{\rho}_{flux}^d = \frac{r}{2}F^d - r\rho^d, \qquad (15)$$

where $F^d = T^{-1}(|1\rangle\langle1| + |2\rangle\langle2|)T$ has three diagonal and six off-diagonal entries. The Bloch equations are most easily handled by moving to the interaction picture, given by $\hat{O} = e^{-i\hat{H}_0 t/\hbar}\tilde{O}e^{i\hat{H}_0 t/\hbar}$, where $\tilde{O}$ is an interaction picture operator.

C. Steady-state solution

The 4×4 matrix equation (12) yields 16 independent equations that we solve in the steady state. Then, the populations in the interaction picture are static, $\dot{\tilde{\rho}}_{\nu\nu} = 0$, and the coherences exhibit sinusoidal precession. In particular, $\tilde{\rho}_{4a} = R_{4a} e^{-i(\Omega-\Delta)t}$, $\tilde{\rho}_{4b} = R_{4b} e^{i\Delta t}$, and $\tilde{\rho}_{4c} = R_{4c} e^{i(\Omega+\Delta)t}$, where the $R_{\mu\nu}$ are time independent, and $\Delta = \omega - \omega_{24}$. The other coherences precess at frequencies $\omega_{\mu\nu} = (E_\mu - E_\nu)/\hbar$. Making these steady-state substitutions, the 16 Bloch differential equations transform to a set of time-independent algebraic equations. We assume that $\omega_C = \omega_{24}$, so that the small cavity pulling shift vanishes. The total maser frequency shift is then given by Δ.

In terms of dressed-basis density matrix elements (rotated out of the interaction picture), the atomic coherence $\rho_{42}(\omega)$ is given by

$$
\rho_{42}(\omega) = \left(\frac{X_{12}}{2\Omega} \rho_{4a} + \frac{\delta}{\Omega} \rho_{4b} - \frac{X_{12}}{2\Omega} \rho_{4c} \right)
$$
$$
= \left(\frac{X_{12}}{2\Omega} R_{4a} + \frac{\delta}{\Omega} R_{4b} - \frac{X_{12}}{2\Omega} R_{4c} \right) e^{i\omega t}, \quad (16)
$$

and the magnetization is found from Eq. (2). Inserting this into Eq. (1), we find the following two conditions which determine the maser amplitude and oscillation frequency:

$$
\mathrm{Re}\left(\frac{X_{12}}{2} R_{4a} + \delta R_{4b} - \frac{X_{12}}{2} R_{4c} \right)
$$
$$
= -|X_{24}| \left(\frac{2 Q_C \Delta}{\omega_C} \right) \left[\frac{(\gamma+r)^2}{r\Omega} \left(\frac{I_0}{I_{th}} \right) \right]^{-1}, \quad (17)
$$

$$
\mathrm{Im}\left(\frac{X_{12}}{2} R_{4a} + \delta R_{4b} - \frac{X_{12}}{2} R_{4c} \right) = -|X_{24}| \left[\frac{(\gamma+r)^2}{r\Omega} \left(\frac{I_0}{I_{th}} \right) \right]^{-1},
$$

where $I_0 = r V_b N$ is the total atomic flux into the maser bulb, and I_{th} is the threshold flux for maser oscillation with our simplified spin-exchange model [2]:

$$
I_{th} = \frac{\hbar V_C (\gamma+r)^2}{4\pi |\mu_{24}|^2 Q_C \eta}. \quad (18)
$$

Here V_C is the cavity volume, and η is a dimensionless filling factor [1,2].

We numerically solve the time-independent algebraic system of 16 Bloch equations plus Eqs. (17) to determine the maser frequency shift Δ as a function of Zeeman detuning δ. We find excellent agreement with the previous theoretical bare-atom analysis [12], within the approximation of equal population decay and decoherence rates. (Note that in practice, these decay rates differ by up to a factor of 2).

IV. PHYSICAL INTERPRETATION

The dressed-state analysis provides a straightforward physical interpretation of the double-resonance maser frequency shift. In the absence of the applied Zeeman field,
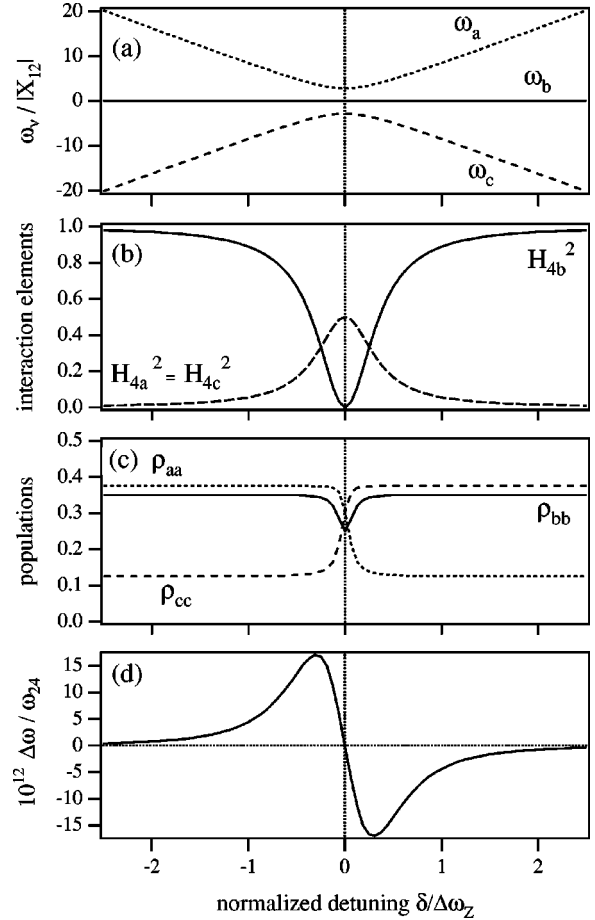

FIG. 4. Calculated dressed-atom quantities plotted against detuning of the applied Zeeman field (in units of Zeeman linewidth, $\Delta\omega_Z = 2\gamma_Z$). The dotted, full, and dashed curves correspond to dressed states $|a\rangle$, $|b\rangle$, and $|c\rangle$, respectively. (a) Dressed-atom frequencies normalized to the Zeeman Rabi frequency. (b) Interaction Hamiltonian matrix elements (squared) from Eq. (13) in units of $\langle 2|\hat{\boldsymbol{\mu}} \cdot \mathbf{H}_C |4\rangle^2$. (c) Steady-state populations of dressed states. (d) Fractional double-resonance maser frequency shift.

atoms injected in bare state $|2\rangle$ are the sole source of the magnetization that provides the positive feedback needed for active oscillation. However, when the near-resonant Zeeman field is applied, it also allows atoms injected in the $m_F = \pm 1$ states (bare states $|1\rangle$ and $|3\rangle$) to contribute via a two-photon process. A dressed-atom interpretation shows how these $m_F = \pm 1$ state atoms can become the dominant source of maser magnetization as the applied Zeeman field nears resonance.

Viewed from the dressed-atom basis, three factors contribute to this interpretation. First, as shown in Fig. 4(a), the applied Zeeman field shifts the energies of the two dressed levels $|a\rangle$ and $|c\rangle$ symmetrically relative to level $|b\rangle$, which remains unperturbed. Second, near the Zeeman resonance, the $\Delta F = 1$ dipole coupling $H_{4b}^2 = \langle 4|\hat{\boldsymbol{\mu}} \cdot \mathbf{H}_C |b\rangle^2$ vanishes, while H_{4a}^2 and H_{4c}^2 become equally dominant, as shown in Fig. 4(b). Third, below resonance ($\delta < 0$) the steady-state population of state $|a\rangle$ is greater than that of state $|c\rangle$ ($\rho_{aa} > \rho_{cc}$), while above resonance ($\delta > 0$) the opposite is true

($\rho_{cc} > \rho_{aa}$), as shown in Fig. 4(c). These dressed-state population differences arise from the fact that atoms in bare state $|1\rangle$ are injected into the maser while those in bare state $|3\rangle$ are not, under normal operation, so in the steady state $\rho_{11} > \rho_{33}$. For large negative Zeeman detunings, $|a\rangle \to |1\rangle$ and $|c\rangle \to |3\rangle$ [see the discussion following Eq. (11)]. The opposite holds for positive detuning, where $|a\rangle \to |3\rangle$ and $|c\rangle \to |1\rangle$.

These three ingredients combine to create the double-resonance shift of the maser frequency, shown in Fig. 4(d). For small negative Zeeman detunings ($|\delta| < 2\gamma_Z$), the excess of ρ_{aa} over ρ_{cc} and the relatively small size of H_{4b}^2 leads to maser oscillation primarily on the $|a\rangle \leftrightarrow |4\rangle$ transition. That is, atoms injected into the maser cavity in bare state $|1\rangle$ contribute significantly to the maser oscillation via a two-photon process: one Zeeman transition photon and one microwave photon within the resonant cavity linewidth. This $|a\rangle \leftrightarrow |4\rangle$ transition is at a slightly higher frequency than in the unperturbed (no applied field) maser, so the maser frequency is increased. Conversely, for small positive Zeeman detunings ($\delta < 2\gamma_Z$), the maser oscillates preferentially on the $|c\rangle \leftrightarrow |4\rangle$ transition, and the maser frequency is decreased. For larger Zeeman detunings (positive or negative), the coupling of state $|4\rangle$ to unshifted dressed state $|b\rangle$ becomes dominant, and the magnitude of the frequency shift is reduced. For zero Zeeman detuning, dressed states $|a\rangle$ and $|c\rangle$ are equally populated in the steady state, and the maser frequency shift exactly vanishes.

Injection of an electronic polarization into the maser bulb is needed for the applied Zeeman field to induce a maser frequency shift. Since ω_a and ω_c are spaced equally about the unperturbed maser frequency ω_b, and since $H_{4a}^2 = H_{4c}^2$, a necessary condition for a maser shift is a difference in the steady-state values of ρ_{aa} and ρ_{cc}, which is a direct consequence of a difference in the injected populations of bare states $|1\rangle$ and $|3\rangle$, i.e., a net electronic polarization.

V. APPLICATION

The double-resonance hydrogen maser technique was originally studied for use in autotuning the maser cavity [12]. In addition to the double-resonance frequency shift, there is a cavity pulling shift for a mistuned maser cavity, with a magnitude dependent on the linewidth of the hyperfine transitions, through the line-Q [see Eq. (5)]. The applied Zeeman radiation depletes the population of bare state $|2\rangle$, thereby increasing the linewidth of the hyperfine transition. Andresen [12] showed that the cavity can be tuned to the atomic frequency by modulating the hyperfine linewidth with applied Zeeman radiation and adjusting the cavity frequency such that there is no modulation of the maser frequency. However, this method requires accurate setting of the applied Zeeman field to the Zeeman resonance (i.e., $\delta = 0$).

The double-resonance technique can also be used for precision Zeeman spectroscopy in a hydrogen maser. Traditionally, the Zeeman frequency in a hydrogen maser operating at low magnetic fields is measured by sweeping an audio frequency field through the Zeeman resonance, and monitoring the maser power. The power is diminished near resonance with a Lorentzian shape with a width on the order of 1 Hz. Typical resolution of the Zeeman frequency with this technique is about 100 mHz. However, by utilizing the sharp, antisymmetric profile of the double resonance frequency shift, the hydrogen Zeeman frequency can be determined with a resolution of about 1 mHz. Recently we used this double-resonance technique in a search for Lorentz symmetry violation of the hydrogen atom's electron and proton spin [19], motivated by a general extension of the standard model of elementary particle physics [20].

VI. CONCLUSION

We used the dressed-atom formalism to calculate the frequency shift of a hydrogen maser induced by an applied field near the $F=1$, $\Delta m_F = \pm 1$ Zeeman transition frequency. The result is in excellent quantitative agreement with previous bare-atom basis calculations [12,15], within a simplified spin-exchange approximation and with equal decay rates for all populations and coherences. The dressed-atom picture provides a simple physical understanding of the double resonance frequency shift, and in particular, the atomic polarization dependence of the frequency shift. The double-resonance technique can be employed in precision spectroscopy of the hydrogen Zeeman frequency, e.g., in a test of Lorentz symmetry of the standard model [19,20].

[1] D. Kleppner, H.M. Goldenberg, and N.F. Ramsey, Phys. Rev. **126**, 603 (1962).

[2] D. Kleppner, H.C. Berg, S.B. Crampton, N.F. Ramsey, R.F.C. Vessot, H.E. Peters, and J. Vanier, Phys. Rev. **138**, A972 (1965).

[3] J. Vanier and C. Audoin, *The Quantum Physics of Atomic Frequency Standards* (Hilger, Bristol, 1989), Chap. 6.

[4] E.N. Fortson, D. Kleppner, and N.F. Ramsey, Phys. Rev. Lett. **13**, 22 (1964).

[5] S.B. Crampton, Phys. Rev. **158**, 57 (1967).

[6] P.F. Winkler, D. Kleppner, T. Myint, and F.G. Walther, Phys. Rev. A **5**, 83 (1972).

[7] R.L. Walsworth, I.F. Silvera, E.M. Mattison, and R.F.C. Vessot, Phys. Rev. A **46**, 2495 (1992).

[8] M.E. Hayden, M.D. Hürlimann, and W.N. Hardy, Phys. Rev. A **53**, 1589 (1996).

[9] R.F.C. Vessot, M.W. Levine, E.M. Mattison, E.L. Blomberg, T.E. Hoffman, G.U. Nystrom, B.F. Farrel, R. Decher, P.B.

Eby, C.R. Baugher, J.W. Watts, D.L. Teuber, and F.D. Wills, Phys. Rev. Lett. **45**, 2081 (1980).

[10] R.L. Walsworth, I.F. Silvera, E.M. Mattison, and R.F.C. Vessot, Phys. Rev. Lett. **64**, 2599 (1990).

[11] R.L. Walsworth and I.F. Silvera, Phys. Rev. A **42**, 63 (1990).

[12] H.G. Andresen, Z. Phys. **210**, 113 (1968).

[13] N.F. Ramsey, Phys. Rev. **100**, 1191 (1955).

[14] H.G. Andresen (unpublished).

[15] J.-Y. Savard, G. Busca, S. Rovea, M. Desaintfuscien, and P. Petit, Can. J. Phys. **57**, 904 (1979).

[16] P.L. Bender, Phys. Rev. **132**, 2154 (1963).

[17] C. Cohen-Tannoudji, J. Dupont-Roc, and G. Grynberg, *Atom-Photon Interactions* (Wiley, New York, 1992), Chap. VI.

[18] We have introduced a factor of $\frac{1}{2}$ to the values for the Rabi frequencies $|X_{24}|$, $|X_{12}|$, and $|X_{23}|$ to account for the use of the rotating-wave approximation.

[19] D.F. Phillips, M.A. Humphrey, E.M. Mattison, R.E. Stoner, R.F.C. Vessot, and R.L. Walsworth, Los Alamos e-print physics/0008230.

[20] R. Bluhm, V.A. Kostelecký, and N. Russell, Phys. Rev. Lett. **82**, 2254 (1999).